BEILSTEIN JOURNAL OF NANOTECHNOLOGY

Supporting Information

for

Ultrasharp gold nanobipyramids: synthetic shape-purity control and SERS-sensitive detection of malachite green

Quang Duy Nguyen, Chau-A Thi Ho, Lo Nu Hoang Tien, Dohoon Lee, Thi Thanh Nguyen Ho, Le Vinh Phong, Vu Thi Hanh Thu, Hai Son Truong-Lam, Khuong Quoc Vo and Sy Van Vu

Beilstein J. Nanotechnol. **2026,** *17,* 1663–1681. doi:10.3762/bjnano.17.115

Additional experimental and characterization data

License and Terms: This is a supporting information file under the terms of the Creative Commons Attribution License (https://creativecommons.org/licenses/by/4.0). Please note that the reuse, redistribution and reproduction in particular requires that the author(s) and source are credited and that individual graphics may be subject to special legal provisions.
The license is subject to the *Beilstein Journal of Nanotechnology* terms and conditions: (https://www.beilstein-journals.org/bjnano/terms)

Table S1: Summary of surface plasmon resonance peaks and bipyramid morphology yield for AuBP with the seed conditions employed while keeping constant growth solution parameters.

Figure	t-SPR (nm)	l-SPR (nm)	[l-SPR]/[t-SPR]	%AuBP
1c	524	701	0.4	14.7%
1d	525	716	2.1	48.5%
1e	534	780	5.2	75.8%
S1	548	801	2.5	58.3%

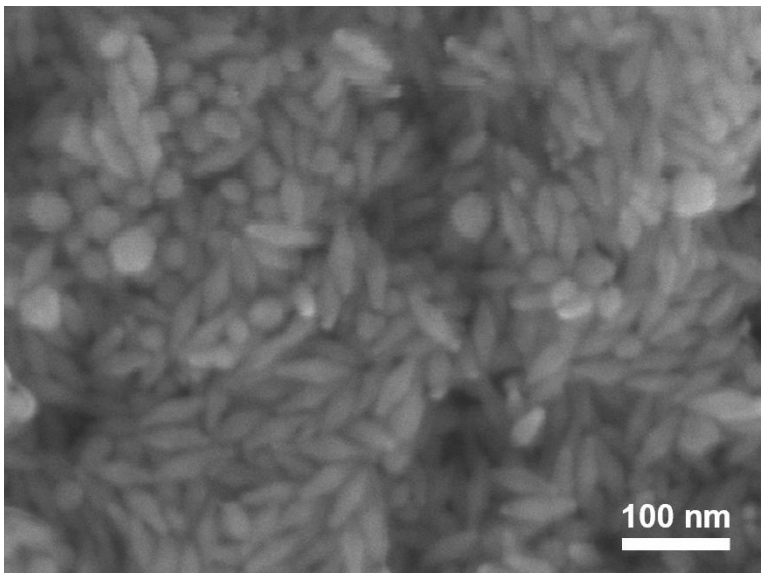

Figure S1: SEM image of AuBP synthesized from seed-CTAB.

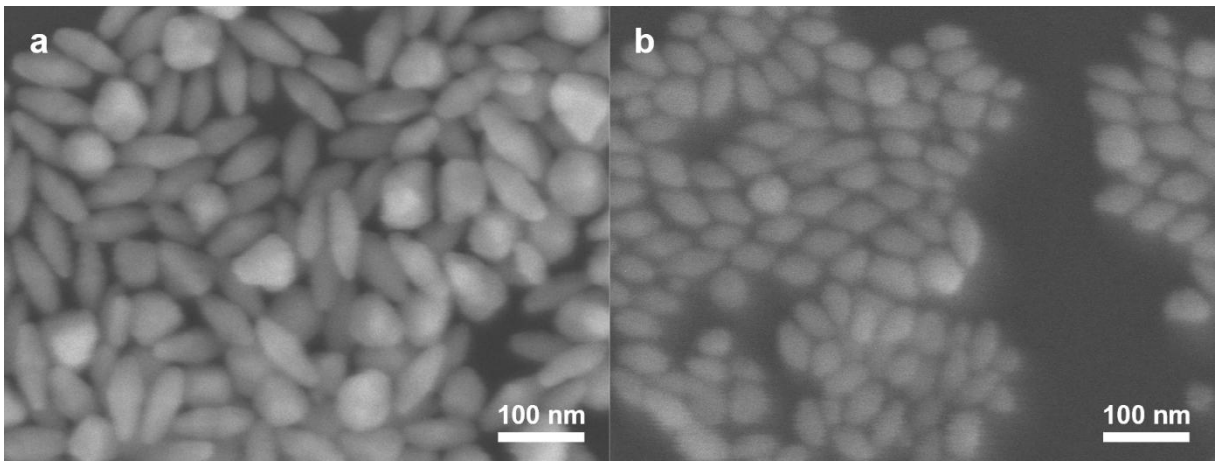

Figure S2: SEM images of AuBP synthesized with different concentrations of CTAB surfactant: **(a)** 50 mM and **(b)** 150 mM.

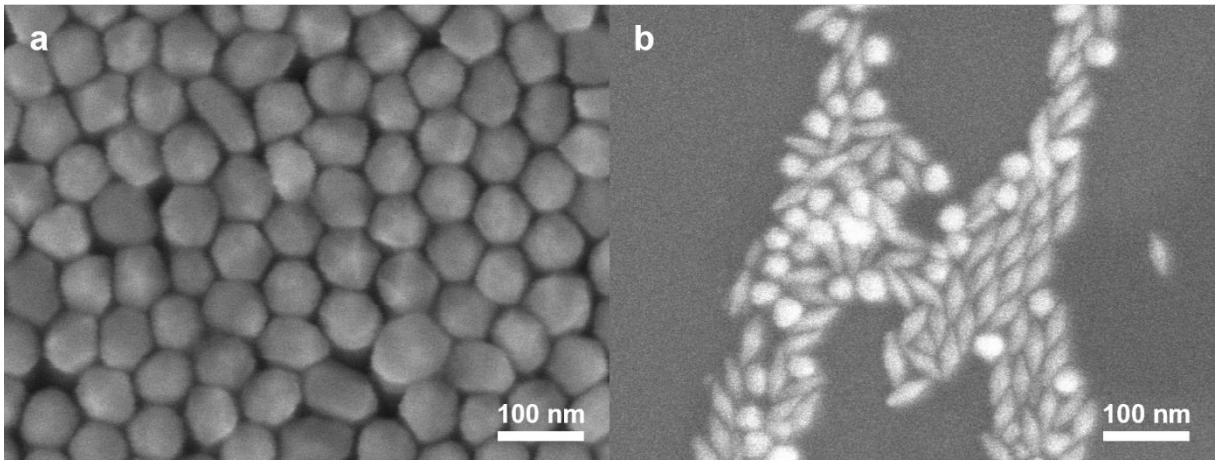

Figure S3: SEM images of AuBP synthesized with different concentrations of $AgNO_3$ **(a)** 0 and **(b)** 0.05 M.

Table S2: Synthesis conditions, sizes, and yields of AuBP synthesized with different seed volumes (**Figure 6**).

Figure	Seed volume (µL)	l-SPR (nm)	Length (nm)	Width (nm)	Aspect ratio	%AuBP
6*a*	750	711	33.9 ± 2.6	14.3 ± 1.4	2.4 ± 0.2	67.2%
6*b*	500	721	42.2 ± 1.8	16.8 ± 1.1	2.5 ± 0.2	70.9%
6*c*	250	742	46.6 ± 1.8	18.1 ± 1.2	2.6 ± 0.2	69.6%
6*d*	150	749	57.0 ± 1.8	21.5 ± 1.6	2.7 ± 0.2	71.5%
6*e*	100	780	60.7 ± 2.4	21.6 ± 1.0	2.8 ± 0.1	75.8%

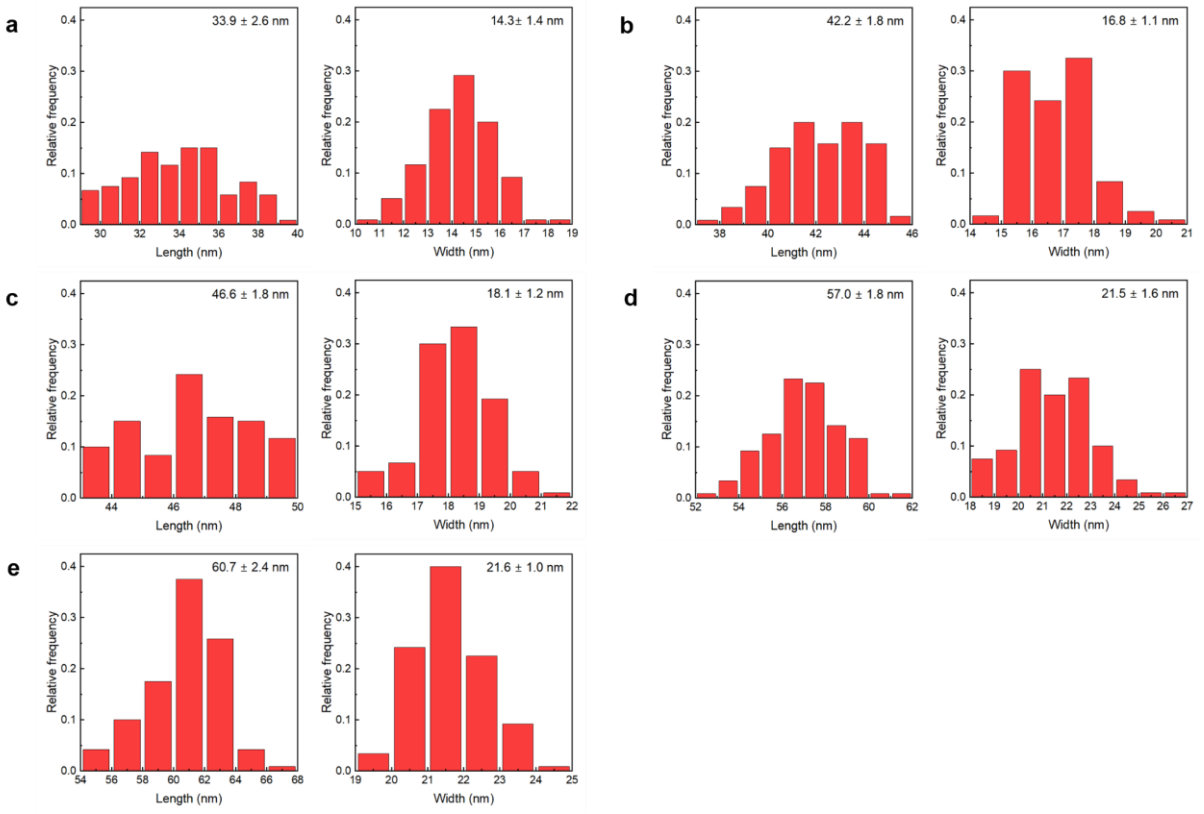

Figure S4: Size distribution of AuBP synthesized with different seed volumes (**Table S2**): **(a)** 750, **(b)** 500, **(c)** 250, **(d)** 150, and **(e)** 100 µL, respectively.

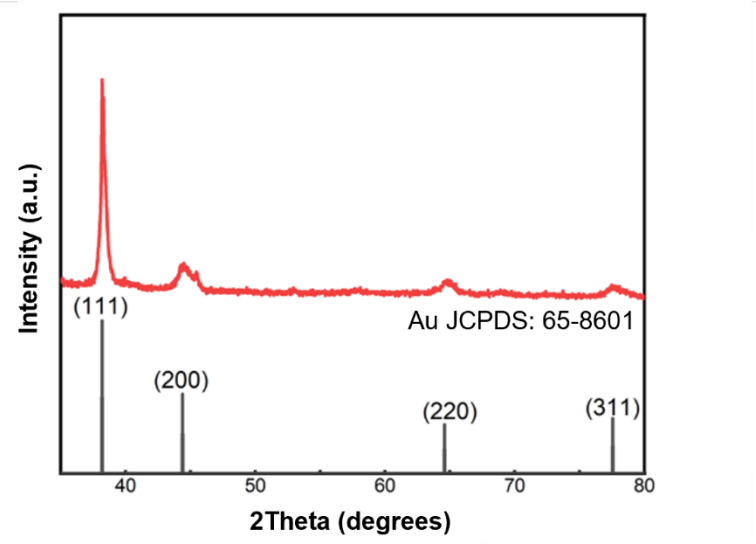

Figure S5: XRD pattern of AuBP.

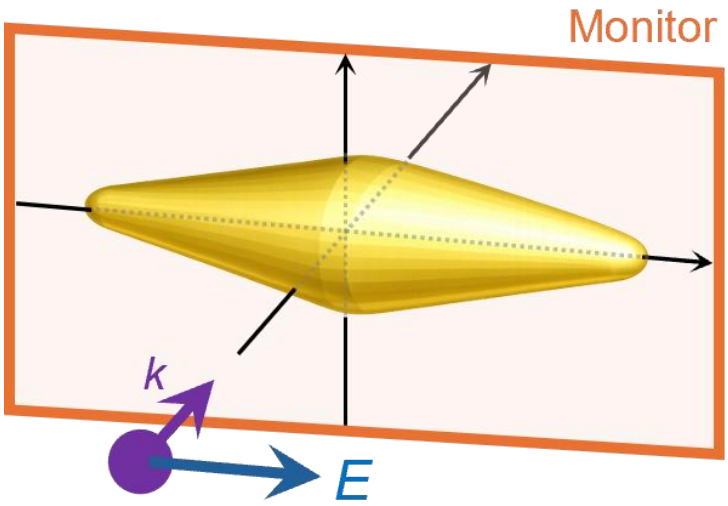

Figure S6: Scheme of the electric field simulation for the AuBP.

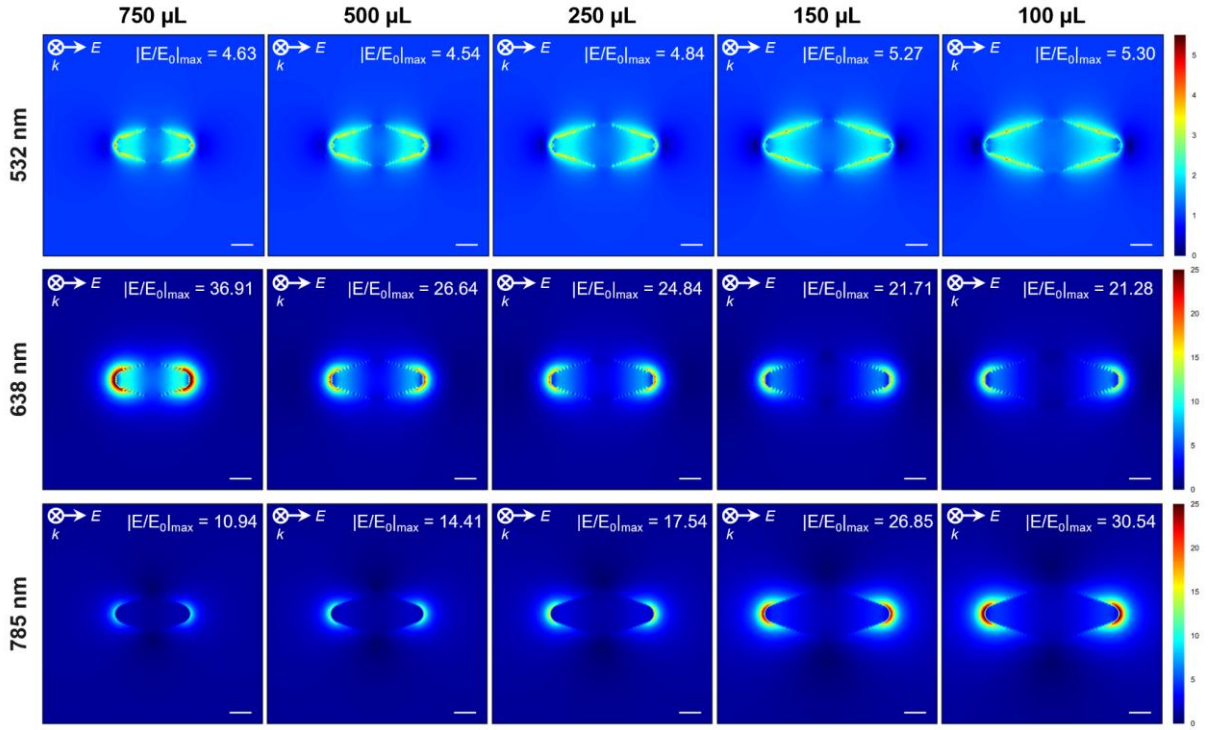

Figure S7: Electric field distribution of the AuBP at experimental Raman excitation wavelengths with 3D models built from different seed-volume average sizes. The refractive index of the medium was set to 1.33 to mimic water.

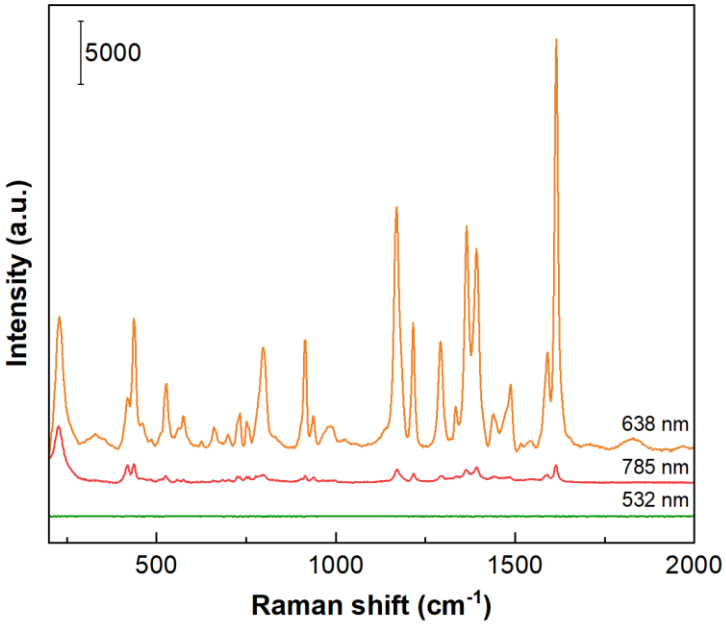

Figure S8: Raman spectra of the AuBP SERS substrate with 10^{-5} M MG using 3 different excitation laser sources at 532 nm, 638 nm, and 785 nm.

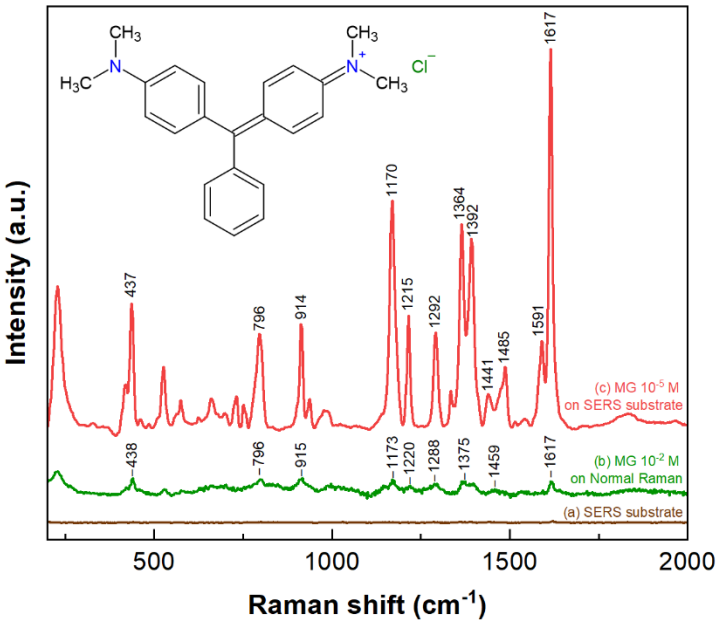

Figure S9: (a) Raman spectra of AuBP substrate. **(b)** 10^{-2} M MG sample onto glass substrate and **(c)** 10^{-5} M MG sample on SERS AuBP substrate.

Enhancement factor determination

The analytical enhancement factor (AEF) is crucial for determining AuBP's signal enhancement capabilities. The AEF value for the SERS performance of AuBP nanosubstrates was calculated using **Equation S1**.

$$\mathrm{AEF} = \frac{\mathrm{I_{SERS}}}{\mathrm{I_{Raman}}} \times \frac{\mathrm{C_{Raman}}}{\mathrm{C_{SERS}}} \quad \textbf{(S1)}$$

Where I_{SERS} and I_{Raman} are the intensities of the SERS signal from MG on AuBP and the Raman signal from the probe molecules on the glass slide, respectively. C_{SERS} of $10^{-9.0}$ M and C_{Raman} of $10^{-2.0}$ M are the concentrations of MG on the AuBP SERS substrate and glass slide, respectively. The intensities of the Raman bands at 1170 cm^{-1} and 1617 cm^{-1} were used to estimate the AEF value.

At Raman shift 1170 cm^{-1}:

$$\mathrm{AEF} = \frac{\mathrm{I_{SERS}}}{\mathrm{I_{Raman}}} \times \frac{\mathrm{C_{Raman}}}{\mathrm{C_{SERS}}} = \frac{109.5}{436.4} \times \frac{10^{-2.0}}{10^{-9.0}} = 2.5 \times 10^{6}$$

At Raman shift 1617 cm^{-1}:

$$\mathrm{AEF} = \frac{\mathrm{I_{SERS}}}{\mathrm{I_{Raman}}} \times \frac{\mathrm{C_{Raman}}}{\mathrm{C_{SERS}}} = \frac{252.5}{650.7} \times \frac{10^{-2.0}}{10^{-9.0}} = 3.9 \times 10^{6}$$

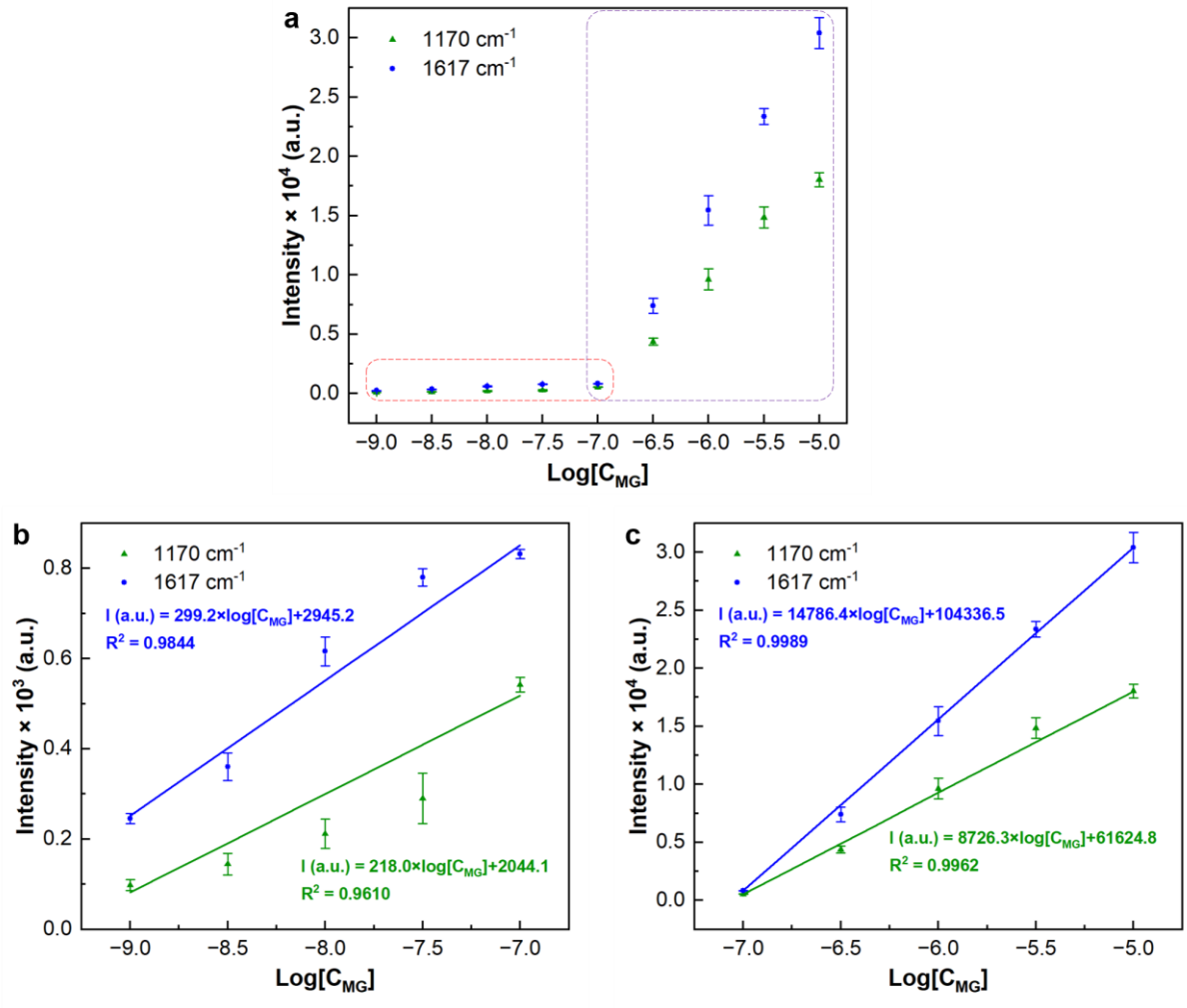

Figure S10: (a) The correlation between the logarithm of MG concentration and Raman peak intensity. The graph illustrates the linear relationship of signal intensity with the logarithm of concentration **(b)** from −9 to −7 and **(c)** from −7 to −5 at 1170 cm^{-1} and 1617 cm^{-1}.

When the MG concentration ranged from 10^{-7} M to 10^{-5} M, two linear equations were obtained: at 1617 cm^{-1}, the linear equation is I (a.u.) = 14786.4×log[C_{MG}] + 104336.5 (R^2 = 0.9989), and at 1170 cm^{-1}, the linear equation is I (a.u.) = 8726.3×log[C_{MG}] + 61624.8 (R^2 = 0.9962). In the lower concentration range from 10^{-7} M to 10^{-9} M, at 1617 cm^{-1}, the linear equation is I (a.u.) = 299.2×log[C_{MG}] + 2945.2 (R^2 = 0.9844), and at 1170 cm^{-1}, the linear equation is I (a.u.) = 218.0×log[C_{MG}] + 2044.1 (R^2 = 0.9610). The high R^2 values of all four calibration curves indicate a good linear response of the SERS signal and meet the requirements for SERS analysis.

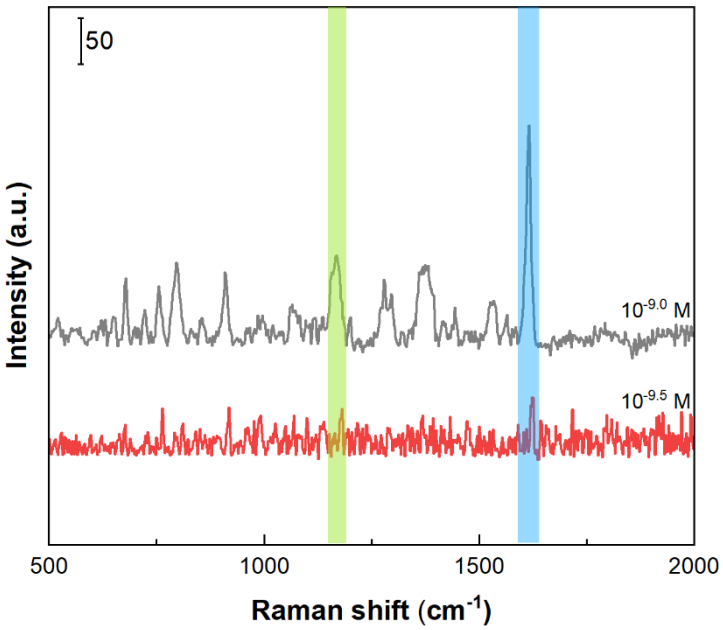

Figure S11: Raman spectra of MG on AuBP substrates at 10^{-9} M and $10^{-9.5}$ M.

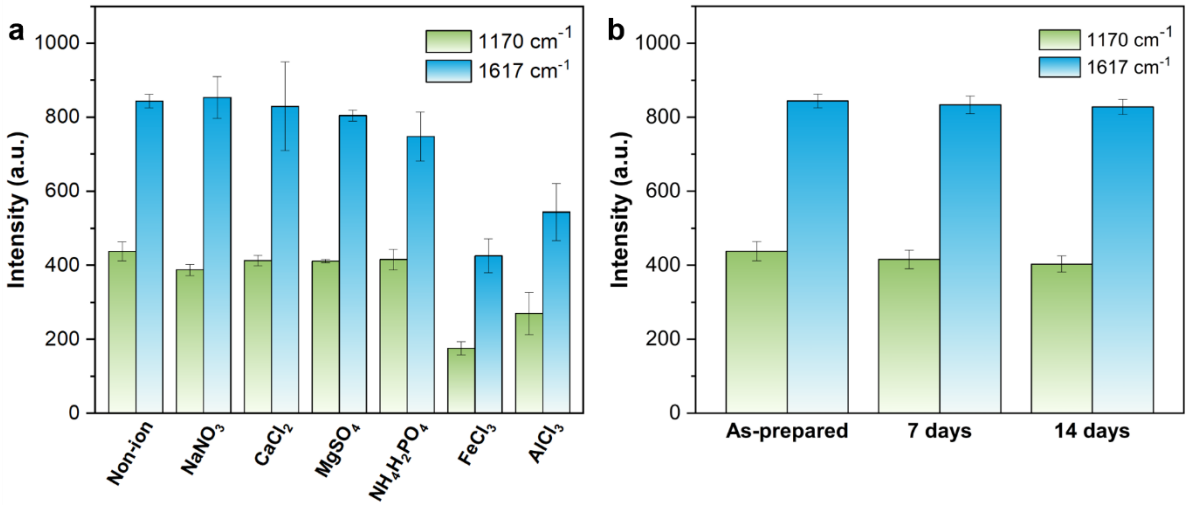

Figure S12: Raman intensity of malachite green at peaks of 1170 cm^{-1} and 1617 cm^{-1} (a) at 10^{-7} M MG in the presence of other inorganic ion solutions at concentrations of 10^{-5} M and **(b)** for the stability test with 10^{-7} M MG after 7 and 14 days.

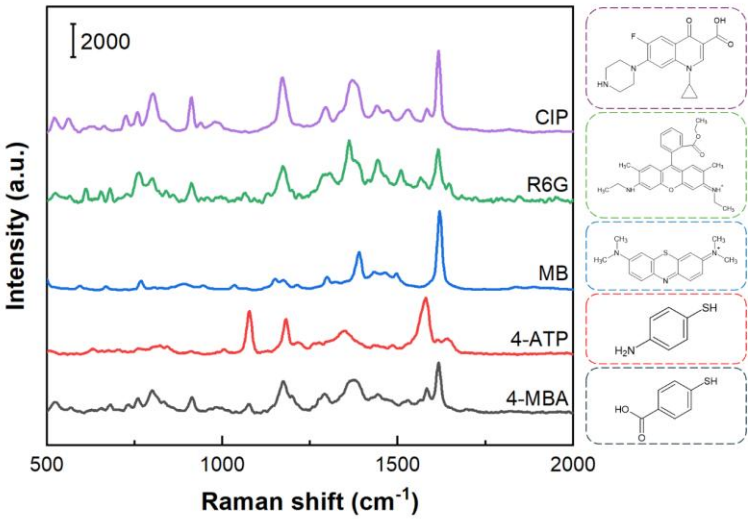

Figure S13: Raman signal enhancement ability of some other chemical molecules onto the AuBP substrate under the same measurement conditions.

Table S3: Assignment for Raman and SERS peaks of malachite green molecules [1,2].

Raman (cm^{-1})	SERS (cm^{-1})	Vibrational assignment
438	437	Phenyl-C-phenyl out-of-plane bending (γ(phenyl-C-phenyl))
796	796	Ring C-H out-of-plane bending ($\gamma(C\text{-}H)_{ring}$)
915	914	C-H out-of-plane bending (γ(C-H))
1173	1170	In-plane aromatic C-H vibration of the ring ($\delta_{in}(C\text{-}H)_{ring}$)
1220	1215	C-H rocking ($\delta(C\text{-}H)_{ring}$)
1288	1292	Aromatic ring C-C stretching ($\nu(C\text{-}C)_{ring}$)
1375	1364	N-phenyl stretching
	1392	$\delta(C\text{-}H)_{ring}$ ($\nu(C\text{-}C)_{ring}$)
1459	1441	$\nu(C\text{-}C)_{ring}$
	1485	C-H bending vibration ($\delta(CH_3)$)
1617	1591	Ring C-C stretching ($\nu(C\text{-}C)_{ring}$)
	1617	Ring C=C stretching ($\nu(C{=}C)_{ring}$)

Table S4: The signal of Raman peak intensity at 1170 cm^{-1} and 1617 cm^{-1} of 10^{-7} M MG at 20 random points onto two AuBP SERS substrates.

Substrate	Spot	Raman peak intensity (a.u.)	
		1170 cm^{-1}	**1617 cm^{-1}**
1st substrate	1	523.61	842.82
	2	548.53	822.95
	3	372.04	809.99
	4	436.68	823.34
	5	459.27	796.64
	6	412.51	850.61
	7	527.67	908.05
	8	553.92	829.58
	9	512.28	769.85
	10	400.41	798.81
2nd substrate	11	455.72	821.80
	12	433.92	717.77
	13	455.63	713.78
	14	496.81	872.44
	15	382.48	802.63
	16	504.05	964.65
	17	522.87	978.76
	18	394.16	932.89
	19	348.77	867.74
	20	464.20	858.29

Table S5: Average intensity, SD, and RSD at Raman peaks of 1170 cm^{-1} and 1617 cm^{-1} of malachite green onto two AuBP SERS substrates.

Calculation	Raman intensity (a.u.)	
	1170 cm^{-1}	**1617 cm^{-1}**
1st substrate (spots 1-10)		
Average intensity (a.u.)	474.7	825.3
SD (a.u.)	66.6	37.5
RSD (%)	14.0	4.5
2nd substrate (spots 11-20)		
Average intensity (a.u.)	445.9	853.1
SD (a.u.)	56.5	92.2
RSD (%)	12.7	10.8
Two substrates (spots 1-20)		
Average intensity (a.u.)	460.3	839.2
SD (a. u.)	61.9	70.0
RSD (%)	13.5	8.3

REFERENCES

1. Kumar, P.; Khosla, R.; Soni, M.; Deva, D.; Sharma, S. K. *Sensors and Actuators B: Chemical* **2017**, *246*, 477-486.
2. Sun, Y.; Zhou, K.; Wang, Y.; Lin, Y.; Wang, W.; Xiong, X.; Zhao, X.; Cui, H.; Liang, M.; Wang, Q.; Yang, S.; Li, L. *Food Chemistry* **2025**, *489*, 144920.